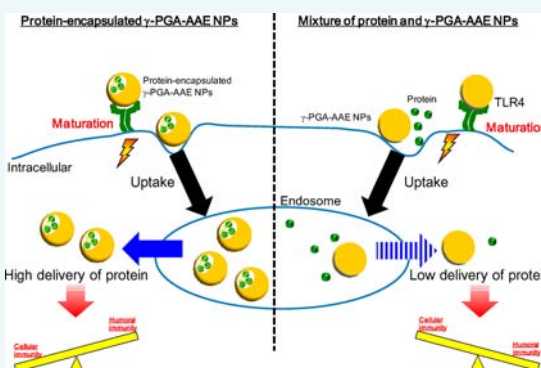


Effect of Hydrophobic Side Chains in the Induction of Immune Responses by Nanoparticle Adjuvants Consisting of Amphiphilic Poly(γ -glutamic acid)

Fumiaki Shima, Takami Akagi, and Mitsuru Akashi*

Department of Applied Chemistry, Graduate School of Engineering, Osaka University, 2-1 Yamada-oka, Suita, Osaka 565-0871, Japan

ABSTRACT: The new generation vaccines are safe but poorly immunogenic, and thus they require the use of adjuvants. Adjuvants that can control the balance and induction level of cellular and humoral immunities are urgently required for the treatment of and/or protection from infectious diseases and cancers. However, there are no adjuvants which can achieve these requirements. In this study, amphiphilic poly(γ -glutamic acid) (γ -PGA) with various kinds of hydrophobic amino acid ethyl esters (AAE) was synthesized (γ -PGA-AAE) and used to prepare antigen-encapsulated nanoparticles (NPs). γ -PGA-graft-Leu (γ -PGA-Leu, where Leu = leucine ethyl ester), γ -PGA-graft-Phe (γ -PGA-Phe, where Phe = phenylalanine ethyl ester), and γ -PGA-graft-Trp (γ -PGA-Trp, where Trp = tryptophan ethyl ester) formed monodispersed NPs that encapsulated ovalbumin (OVA). The type and the induction level of the antigen-specific cellular and humoral immunities could be controlled by the kinds of hydrophobic segments and vaccine formulation (encapsulation or mixture) used. When OVA was encapsulated into NPs, the cellular immunity was dominantly induced, while humoral immunity was dominant when OVA was mixed with NPs. These results are a first report to demonstrate that the balance and induction level of cellular and humoral immunities could be controlled by modifying compositions of NPs and vaccine formulation. Our results suggest that γ -PGA-AAE NPs can provide safe and efficient nanoparticle-based vaccine adjuvants, and the results also provide guidelines in the rational design of amphiphilic polymers as vaccine adjuvants which can control the balance of immune responses.



INTRODUCTION

Vaccination protects against infectious diseases and cancers by inducing strong immune responses. Until now, various antigens have been developed such as attenuated pathogens, whole inactivated organisms, and inactivated bacterial toxins, though they require labor-intensive production processes and often suffer from toxicity and immunogenicity. Recently, next-generation antigens such as subunits, recombinant proteins, and synthetic peptides have been employed to develop safe and efficient vaccine systems. Although these antigens are generally safe, they are often poorly immunogenic. Therefore, a vaccine adjuvant which ensures both safety and antigen delivery system is eagerly required for the induction of potent immune responses.¹ These adjuvants possess two functions: antigen delivery and immune stimulation.² They deliver antigens to antigen presenting cells (APCs) such as dendritic cells (DCs) and macrophages, and induce immune responses. Recently, “immunoengineering” has been attracted many researchers to develop next-generation vaccine systems.^{3,4} This offers the design of carriers including polymeric nanoparticles (NPs), dendrimers, and liposomes whose components are made of biocompatible or biodegradable polymers.⁵ They can load various antigens, and they are taken up by APCs, which initiates an antigen-specific immune response.^{6,7} For the induction of immune responses, the intracellular behavior of antigens in

APCs is essential. The antigens are usually localized into endosomes after cellular uptake by APCs, and they are degraded to peptides and subsequently present on APC surfaces.⁸ Humoral immunity, which produces antibodies that protect against infection, is induced after presentation of the antigens in endosomes via major histocompatibility complex (MHC) class II. On the other hand, cellular immunity, which kills infected cells by inducing antigen-specific cytotoxic T lymphocytes (CTLs), is induced after presentation of antigens, which escape from endosomes and are processed by proteasomes, via MHC class I.⁹ These observations suggest that the type and the induction level of antigen-specific cellular and humoral immunities could be manipulated by controlling the antigen behavior (cellular uptake, maturation, biodistribution). Manipulation of the immune responses could provide novel vaccine strategies against infectious diseases, and also provide new treatment methods for cancer, allergies, and autoimmune diseases. However, there are no adjuvants and vaccine carriers which can manipulate the balance of immune responses. For the development of a vaccine adjuvant which can control a balance of immune responses, NPs are one of the

Received: February 23, 2015

Revised: March 23, 2015

Published: April 12, 2015



greatest candidates, as their physicochemical properties (size, hydrophilic/hydrophobic balance, compositions) are easily and precisely controlled. With a greater mechanistic understanding of the interactions between vaccine carriers and immune cells, significant efforts have been paid to target and manipulate immune responses.² Recently, several reports have revealed that the hydrophobicity of particulate adjuvants and antigens is a key factor for initiating immune responses.^{10,11} The hydrophobicity of NPs drastically influenced their interaction with the cells, and thus the consequent immune responses.^{12,13} Moreover, the interactions between polymers and cell membranes were affected by the hydrophobicity of the polymers,^{14,15} which suggested that the intracellular behavior of antigens may be controlled by engineering polymer composition. Since controlling the antigen behavior in cells is essential for the induction of antigen-specific immune responses, we may be able to manipulate them by varying the composition (hydrophobicity, type of hydrophobic segments) of polymers which are contained in NPs.

In a previous study, amphiphilic copolymers composed of poly(γ -glutamic acid) (γ -PGA) as the hydrophilic backbone and L-phenylalanine ethyl ester (Phe) as hydrophobic segments (γ -PGA-Phe) were synthesized and NPs were prepared from them to develop nanoparticle-based vaccine adjuvants.^{16,17} The encapsulated antigen into γ -PGA-Phe NPs was efficiently taken up by APCs, which resulted in the induction of the potent antigen-specific immune response.¹⁸ We showed that γ -PGA-Phe NPs could stimulate APCs via Toll-like receptor (TLR) 4 due to their adjuvant effect.^{19,20} We also reported that γ -PGA-Phe NPs possess membrane-disruptive activities at endosomal pH, and escaped from endosomes after they were located there.²¹ Recently, we reported that the hydrophobicity of γ -PGA-Phe NPs (grafting degree of Phe) significantly affected interactions with immune cells (membrane disruptive activity, cellular uptake, and maturation of DCs), and consequent antigen-specific immune responses.^{22,23} On the other hand, it has been reported that individual amino acids have different hydrophobicity.^{24,25} In addition, membrane-disruptive synthetic peptides containing both hydrophobic NPs and various amino acids, which are activated at endosomal pH, have been developed.^{26,27} Therefore, the sequence and/or types of amino acids are crucial for interactions between cells and vaccine carriers. These data suggest that interactions of NPs with APCs could be controlled by changing the type of hydrophobic segment, such as hydrophobic amino acids grafted to polymers, and thus could achieve the manipulation of immune responses.

In this study, for the manipulation of antigen-specific immune responses, amphiphilic γ -PGA copolymers, which were grafted with various types of amino acid ethyl esters (AAE) as hydrophobic segments (γ -PGA-AAE), were synthesized, and protein-encapsulated γ -PGA-AAE NPs were prepared from the aforementioned copolymers. The relationships between the hydrophobic segment of γ -PGA-AAE NPs and the cellular uptake of encapsulated proteins, the maturation of DCs, and the induction of antigen-specific cellular/humoral immunity were investigated. Our results demonstrated that the hydrophobic segment of γ -PGA-AAE NPs is a key factor to control interactions with DCs, and thus we successfully manipulated the balance and induction level of antigen-specific cellular and humoral immunities.

RESULTS AND DISCUSSION

Synthesis and Preparation of Protein-Encapsulated γ -PGA-AAE NPs. Amphiphilic γ -PGA-AAE copolymers were synthesized by coupling reactions between amine groups of AAE and carboxylic groups in γ -PGA using EDC. Grafting degrees of AAE were determined by ¹H NMR using integrals of γ -PGA and AAE. Grafting degrees of Leu, Phe, and Trp were 87%, 50%, and 71%, respectively. These grafting degrees were selected to avoid the influence of the surface hydrophobicity of NPs. The surface hydrophobicity of γ -PGA-AAE NPs was evaluated by measuring contact angles of γ -PGA-AAE copolymers. Liu et al. evaluated the surface hydrophobicity of microparticles by measuring the contact angles of copolymers spin coated on glass substrates, and demonstrated that there was a correlation between surface hydrophobicity of microparticles and immune responses.³² In this study, γ -PGA-AAE copolymers were coated on glass substrates and contact angles were measured by dropping deionized water. The contact angles of γ -PGA-AAE copolymers showed almost same values by controlling the grafting degrees of AAEs (Figure 1). The

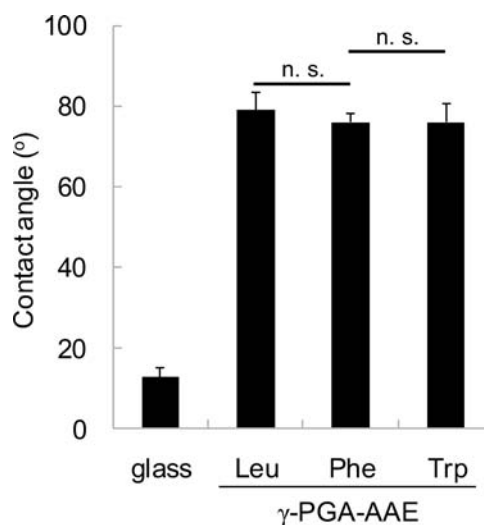


Figure 1. Evaluation of the hydrophobicity of γ -PGA-AAE copolymers by measuring contact angles. γ -PGA-AAE (10 mg/mL in HFIP) was coated on a glass substrate with a spin coater. Contact angles were measured by dropping deionized water (10 drops/sample). The data represent mean \pm SD in each group.

contact angles of γ -PGA-Leu, γ -PGA-Phe, and γ -PGA-Trp were $79 \pm 4^\circ$, $76 \pm 2^\circ$, and $76 \pm 5^\circ$, respectively. These copolymers were used to prepare γ -PGA-AAE NPs and OVA-NPs for the following experiments.

In this study, ovalbumin (OVA) or FITC-labeled OVA (FITC-OVA) was used as a model antigen for evaluating antigen-specific immune responses and cellular uptake. To prepare the OVA-NPs or FITC-OVA-NPs, γ -PGA-AAE copolymers were dissolved in DMSO at a concentration of 10 mg/mL. These solutions were then added to NaCl solutions containing OVA or FITC-OVA, and OVA-NPs or FITC-OVA-NPs were prepared. γ -PGA-AAE copolymers could form NPs due to their intra-/intermolecular hydrophobic interactions. In this study, we adjusted the size of γ -PGA-AAE NPs, OVA-NPs, and FITC-OVA-NPs to 200 nm by changing the NaCl concentration from 0.1 to 0.35 M to eliminate the size effect of γ -PGA-AAE NPs on the interaction with cells and on the immune response. When the grafting degree of AAE was low, a

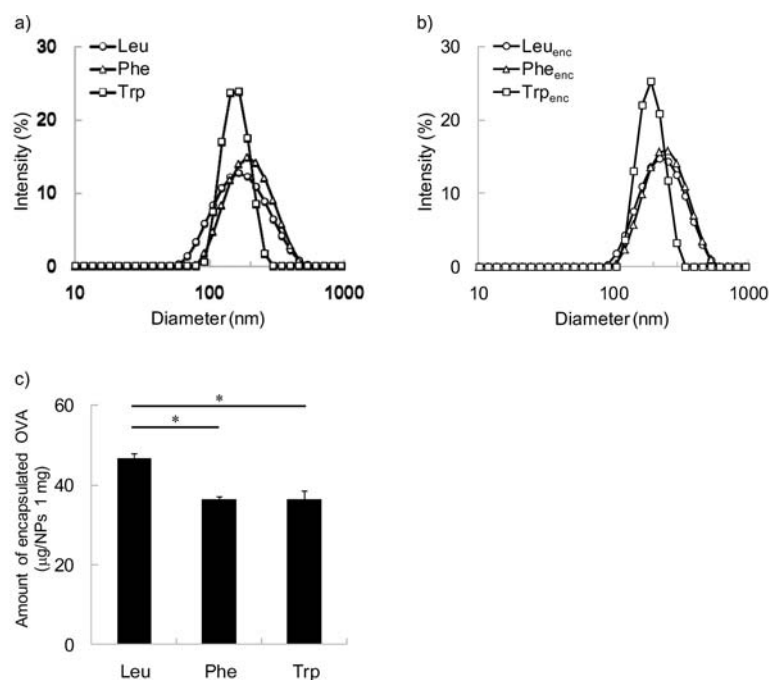


Figure 2. (a) Size distributions of γ -PGA-AAE NPs. (b) Size distributions of OVA-NPs. (c) Entrapped amount of OVA-NPs prepared at various hydrophobic side chains. The particle size in PBS was measured by DLS ($n = 3$). The amount of entrapped OVA was measured by the Lowry method ($n = 3$). γ -PGA-AAE (10 mg/mL in DMSO) was added to equal volume of 875 μ g/mL OVA. To regulate the size of the OVA-NPs, the NaCl concentration was varied from 0.035 to 0.35 M. * $p < 0.01$.

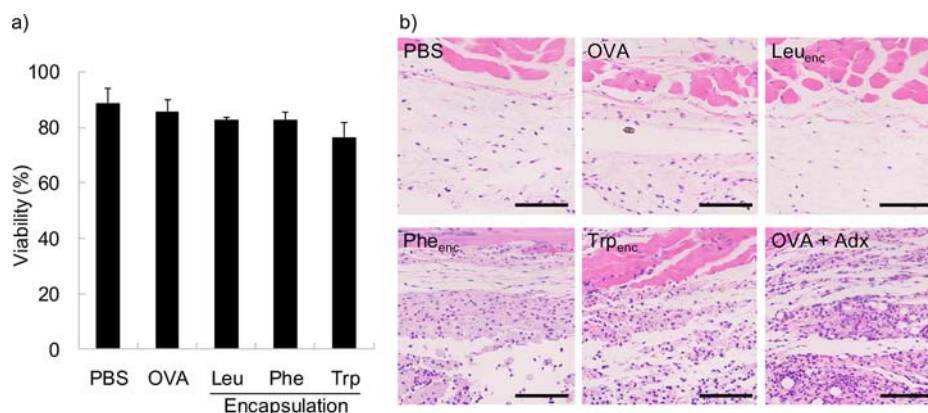


Figure 3. (a) Viability of OVA-NPs. DCs were incubated with OVA-NPs (20 μ g/mL OVA, 500 μ g/mL NPs) of various hydrophobic side chains for 24 h at 37 °C. Cells were then stained with trypan blue dye, and the viability was evaluated. Data are expressed as mean \pm SD in each group ($n = 3$). (b) The effect of hydrophobic side chains of OVA-NPs on *in vivo* inflammatory responses. Mice were injected subcutaneously with OVA-NPs. After 14 days, subcutaneous tissues were collected, fixed, stained with hematoxylin and eosin, and evaluated for inflammatory responses. The original magnifications of these photographs are 40 \times . Scale bars represent 100 μ m.

higher NaCl concentration was needed (0.35 M for γ -PGA-Phe). On the other hand, a low NaCl concentration was enough for the preparation of OVA-NPs or FITC-OVA-NPs with higher grafting degrees (0.1 M for γ -PGA-Leu and γ -PGA-Trp). These were due to the amphiphilic balance and electrostatic repulsion of carboxyl groups in γ -PGA-AAE. Since γ -PGA-AAE with lower grafting degrees possessed fewer hydrophobic moieties and a larger number of carboxyl groups, it required a higher amount of NaCl to reduce electrostatic repulsion of γ -PGA-AAE. On the other hand, γ -PGA-AAE with higher grafting degrees possessed more hydrophobic moieties and a lesser number of carboxyl groups, and required a lower amount of NaCl to form NPs. The size distributions of γ -PGA-AAE NPs, OVA-NPs and the amount of

encapsulated OVA into γ -PGA-AAE NPs are shown in Figure 2. γ -PGA-AAE NPs and OVA-NPs of various AAEs showed monodispersed 200 nm-sized NPs (Figure 2a,b). The zeta potentials of OVA-NPs were negative for all AAE, while the values were different: -19 ± 2 mV for Leu_{enc}, -25 ± 1 mV for Phe_{enc}, and -28 ± 1 mV for Trp_{enc}. The amount of encapsulated OVA into γ -PGA-Leu NPs was slightly higher, while γ -PGA-Phe NPs and γ -PGA-Trp NPs encapsulated almost the same amount (Figure 2c). The encapsulation efficiency was $53 \pm 1\%$ for Leu_{enc}, $42 \pm 1\%$ for Phe_{enc}, and $42 \pm 2\%$ for Trp_{enc}. The size distributions of FITC-OVA-NPs and the amount of encapsulated FITC-OVA into γ -PGA-AAE NPs were almost the same as those of OVA-NPs (data not shown).

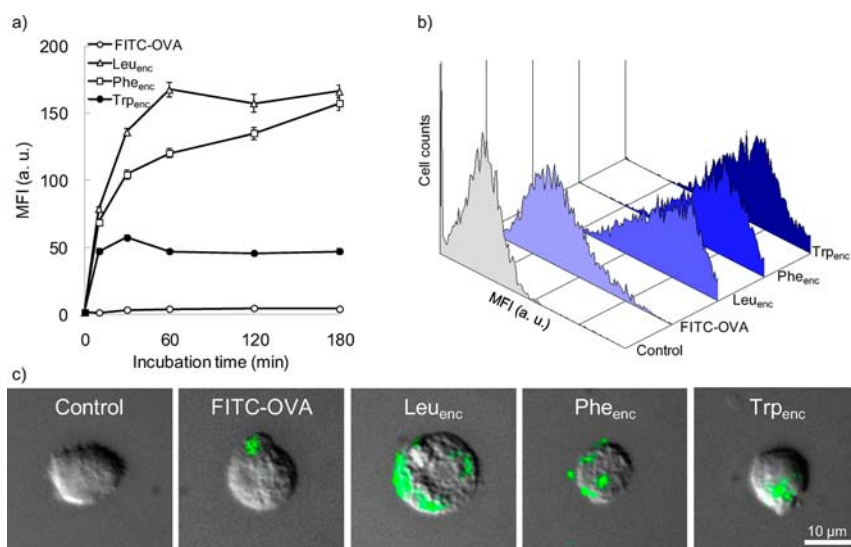


Figure 4. (a) Cellular uptake of FITC-OVA-NPs by DCs. Cells were incubated with FITC-OVA (4 μg/mL) or FITC-OVA-NPs (4 μg/mL FITC-OVA, 100 μg/mL NPs) of various hydrophobic segments for predetermined time periods at 37 °C. The uptake amount was measured by flow cytometry. The data are expressed as the mean fluorescence intensity \pm SD in each group ($n = 3$). (b) Histogram of the cellular uptake of FITC-OVA or FITC-OVA-NPs by DCs incubated for 180 min at 37 °C. (c) Representative fluorescence microscopic images of the cellular uptake of FITC-OVA or FITC-OVA-NPs. Cells were observed using confocal fluorescence microscopy.

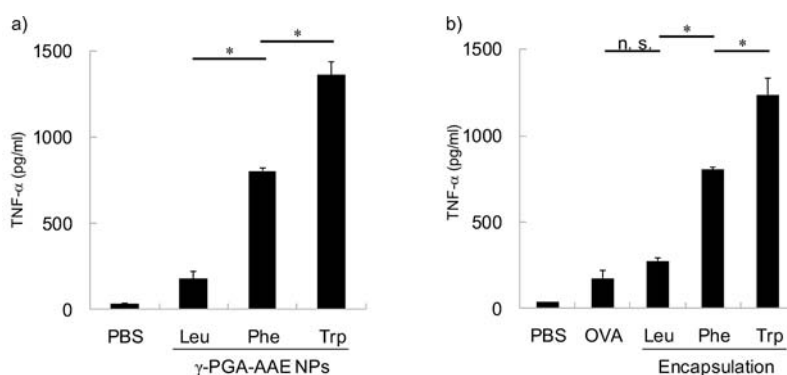


Figure 5. Induction of inflammatory cytokines by (a) γ-PGA-AAE NPs or (b) OVA-NPs. DCs were incubated with (a) γ-PGA-AAE NPs (500 μg/mL) or (b) OVA (20 μg/mL) or OVA-NPs (20 μg/mL OVA, 500 μg/mL NPs) with various hydrophobic side chains for 24 h at 37 °C. Culture supernatants were collected, and cytokines (TNF-α) were measured by ELISA. Data are expressed as mean \pm SD in each group ($n = 3$). * $p < 0.01$.

Cytotoxicity is a critical factor for use of these NPs *in vitro* and *in vivo* experimentations. Therefore, DCs incubated with γ-PGA-AAE NPs or OVA-NPs were stained with trypan blue dye and viability was evaluated. OVA-NPs of various AAEs showed high viabilities, about 80% at 500 μg/mL for NPs and 20 μg/mL for OVA which were comparable to untreated DCs (Figure 3a). γ-PGA-AAE NPs also showed high viabilities, about 80% at 500 μg/mL (data not shown). To evaluate the biocompatibility of OVA-NPs *in vivo*, OVA-NPs were administered subcutaneously. In subcutaneous tissues of mice injected with PBS, OVA, Leu_{enc}, Phe_{enc}, Trp_{enc}, and OVA + Adx, there was no tissue injury such as skin hyperplasia, eschar, or ulcer. On the other hand, subcutaneous tissues which were administered with Phe_{enc}, Trp_{enc}, and OVA + Adx showed inflammatory cell infiltration (Figure 3b). It has been reported that the injection of cationic liposomes resulted in large cell infiltration including monocytes, macrophages, and natural killer cells at injection sites, efficiently stimulating the immune system.^{33,34} Therefore, inflammation at the site of injection of OVA-NPs may be a factor responsible for antigen-specific immune responses.

Cellular Uptake of FITC-OVA-NPs by DCs. To evaluate the effect of hydrophobic segments of γ-PGA-AAE NPs on the cellular uptake of antigen-encapsulated γ-PGA-AAE NPs, DCs were incubated with FITC-OVA-NPs at 37 °C. The fluorescence intensity obtained by flow cytometry demonstrated that encapsulated FITC-OVA was efficiently taken up into cells, while the uptake amount of free FITC-OVA alone was low (Figure 4a). The uptake amount of the encapsulated FITC-OVA into γ-PGA-Leu NPs and γ-PGA-Phe NPs increased in a time dependent manner, whereas those in γ-PGA-Trp NPs reached a plateau within 60 min. Hydrophobic segments of γ-PGA-AAE NPs affected the uptake speed. γ-PGA-Leu NPs and γ-PGA-Trp NPs reached a plateau after 1 h, while γ-PGA-Phe NPs did not (Figure 4b). Hydrophobic segments also affected the uptake amount of encapsulated FITC-OVA. The uptake amount of FITC-OVA encapsulated into γ-PGA-Trp NPs was about 50 times higher than FITC-OVA alone. On the other hand, the uptake amount of FITC-OVA encapsulated into γ-PGA-Leu NPs and γ-PGA-Phe NPs was about 3 times higher than that in γ-PGA-Trp NPs. As the contact angles of γ-PGA-AAE copolymers showed similar

values (Figure 1), which indicated that the type of hydrophobic side chains might affect the cellular uptake of OVA-NPs by DCs. The cellular uptake of FITC-OVA-NPs was also observed with confocal fluorescence microscopy, which showed that the FITC-OVA alone and FITC-OVA-NPs were taken up by DCs and localized inside cells (Figure 4c).

Stimulation of DCs by γ -PGA-AAE NPs and OVA-NPs.

The activation potentials of γ -PGA-AAE NPs or antigen encapsulated γ -PGA-AAE NPs and their relationship to hydrophobic segments were evaluated by measuring tumor necrosis factor (TNF)- α , which is known as a proinflammatory cytokine.³⁵ DCs were incubated with γ -PGA-AAE NPs or OVA-NPs, and the amount of TNF- α secreted in supernatants was measured. As shown in Figure 5a, the activation potential of γ -PGA-AAE NPs was significantly affected by the hydrophobic segment. γ -PGA-Trp NPs showed about 8 times higher secretion of TNF- α than γ -PGA-Leu NPs. Phe_{enc} and Trp_{enc} also significantly stimulated DCs to secrete a large amount of TNF- α as compared with OVA alone, while the activation potential of Leu_{enc} was comparable to the OVA alone (Figure 5b). The activation potential of OVA-NPs of various AAEs showed the same tendency as that of γ -PGA-AAE NPs. We also measured costimulatory molecule (CD) 40 on the DCs by flow cytometry. The expression level of CD40 which was stimulated by OVA-NPs showed same tendency as the secretion level of TNF- α which was stimulated by OVA-NPs (data not shown). It has been reported that the hydrophobicity of NPs drastically affects the immune response.¹³ In a previous study, we revealed that the hydrophobicity of γ -PGA-Phe NPs (grafting degree of Phe) significantly affected the activation level of DCs, which was proportional to the hydrophobicity.²² Tayar et al. also reported that each amino acid has different hydrophobicity (logP); tryptophan (−1.15) > phenylalanine (−1.44) > leucine (−1.72).²⁴ In Figure 5, the activation potential of γ -PGA-AAE NPs and OVA-NPs was γ -PGA-Trp NPs > γ -PGA-Phe NPs > γ -PGA-Leu NPs and Trp_{enc} > Phe_{enc} > Leu_{enc}, which demonstrated that there is good correlation between activation potential of γ -PGA-AAE NPs and the hydrophobicity of each amino acid. As the surface hydrophobicity of γ -PGA-AAE NPs was almost same regardless of hydrophobic segments, it suggests that the hydrophobic segments in NPs may affect the activation of DCs. Although, there had no correlation between cellular uptake and activation potential of OVA-NPs, might be due to differences in the stimulation behavior of OVA-NPs. In a previous study, we reported that γ -PGA-Phe NPs stimulates DCs via TLR4.¹⁹ It has been reported that γ -PGA stimulated APCs via TLR4, which results in the induction of innate immunity and antitumor activity.³⁵ It has also been reported that TLR4 possesses hydrophobic regions and can bind to many different types of hydrophobic parts that initiate innate immune responses.¹¹ Taken altogether, it suggests that γ -PGA-AAE NPs stimulate DCs via TLR4 with different degrees which are derived from differences in the hydrophobicity of grafted side chains, and thus results in differences in the secretion of TNF- α .

Induction of Antigen-Specific Immune Response by OVA-NPs of Various AAEs. As shown above, hydrophobic segments affected the activation of DCs. Therefore, the effect of hydrophobic segments on the induction of antigen-specific cellular immunity was evaluated *in vivo*. OVA-NPs or OVA + NPs of various AAEs were injected subcutaneously to mice on days 0 and 7, their spleens were harvested on day 14, and the immune stimulatory potential was evaluated by measuring

interferon (IFN)- γ producing cells with an enzyme-linked immunospot (ELISPOT) assay. Lymphocytes isolated from spleens were stimulated with an OVA_{257–264} CTL epitope peptide, and OVA_{257–264}-specific IFN- γ -producing cells were determined. OVA-NPs could efficiently induce higher antigen-specific cellular immunity than OVA + Adx (Figure 6). In this

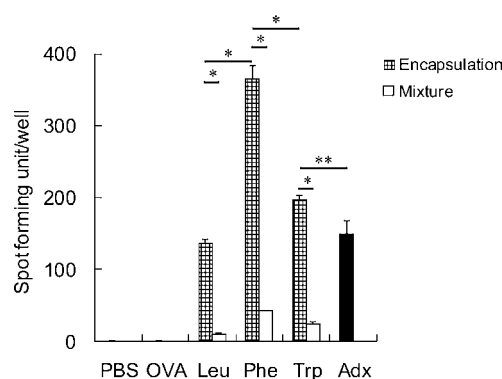


Figure 6. Antigen-specific IFN- γ producing T cells induced by (a) OVA-NPs or (b) OVA + NPs. Spleen cells (2×10^5 cells/well) of mice immunized with the indicated samples were stimulated with OVA_{257–264} peptide (10 μ g/mL) and evaluated for IFN- γ production by ELISPOT. Data are expressed as the number of IFN- γ positive spots per well. The data represent means \pm SD in each group ($n = 3$). * $p < 0.01$, ** $p < 0.05$.

study, Adx was used as a control. The hydrophobic segments drastically affected the induction level of the cellular immunity: the value for Phe_{enc} was about 2.5-fold higher than that for OVA + Adx, while that for Leu_{enc} was comparable to that for OVA + Adx. The cellular immunity was also induced with OVA + NPs, although the induction level was lower than those with OVA-NPs and OVA + Adx (Figure 6). We also evaluated the amount of produced antigen-specific antibodies (Abs). In this study, immunoglobulins IgG and IgE were determined.

IgE Ab, which is known as the cause of allergies, was not detected from all samples, suggesting that OVA-NPs and OVA + NPs were relatively safe vaccine systems (data not shown). OVA-NPs and OVA + NPs produced OVA-specific IgG Ab, while the amount produced was lower than with OVA + Adx (Figure 7). Leu_{enc} suppressed the production of IgG Ab compared with OVA alone. The amount of IgG Ab produced by OVA + NPs tended to be higher than that produced by

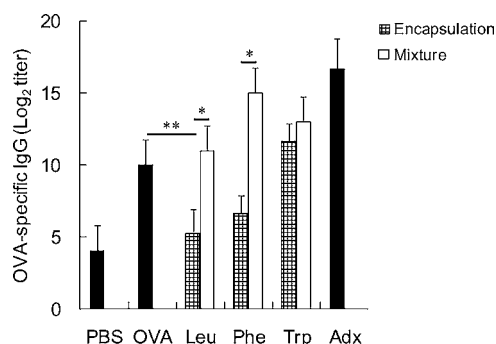


Figure 7. Antigen-specific serum Ab induced by OVA-NPs or OVA + NPs. Sera were analyzed for anti-OVA IgG Ab titers determined by ELISA (8 to 262 144 times dilution). The results represent mean \pm SD of end point titers for three mice ($n = 3$). * $p < 0.01$, ** $p < 0.05$.

OVA-NPs. Interestingly, the balance of the antigen-specific immune response was controlled by antigen formulation (encapsulation or mixture) and the kinds of hydrophobic segments (Figure 8). In Figure 8, the x -axis represents the

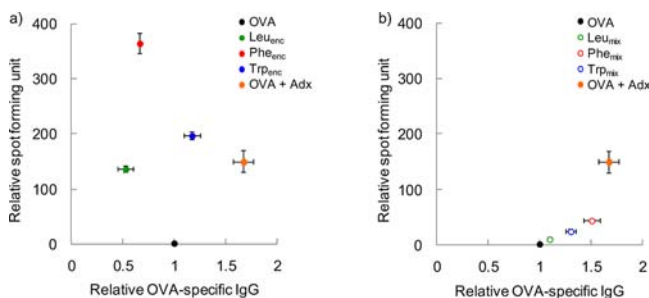


Figure 8. Manipulation of the balance of antigen-specific cellular/humoral immunity by (a) OVA- NPs or (b) OVA + NPs. The x -axis represents the relative amount of OVA-specific IgG Ab by OVA-NPs or OVA + NPs to OVA alone. The y -axis represents the relative spot forming unit of produced IFN- γ by OVA-NPs or OVA + NPs to OVA alone. The plot located in the upper left means that the antigen-specific cellular immunity-biased immune response is induced. The plot located in the lower right means that the antigen-specific humoral immunity-biased immune response is induced.

relative produced amount of OVA-specific IgG by OVA-NPs or OVA + NPs to OVA alone. The y -axis represents the relative spot forming unit of produced IFN- γ by OVA-NPs or OVA + NPs to OVA alone. The plot located in the upper left indicates that the antigen-specific cellular immunity-biased immune response is induced. The plot located in the lower right means that the antigen-specific humoral immunity-biased immune response is induced. The antigen-specific cellular immunity-biased immune response was induced when the antigen was encapsulated into γ -PGA-AAE NPs (Figure 8a), while humoral immunity-biased immune response was induced when the antigen was mixed with γ -PGA-AAE NPs (Figure 8b). The induction level of the immune response was changed by varying the kinds of hydrophobic segments; Phe_{enc} induced the highest cellular immunity, whereas Leu_{enc} induced the lowest, while Leu_{enc} induced the cellular immunity-biased immune response as the plot of Leu_{enc} located in the most left side of OVA in Figure 8a compared with Phe_{enc} and Trp_{enc}. These results may be due to differences in the behavior of antigens at the injection site, interactions between OVA-NPs or OVA + NPs and APCs, especially the intracellular behaviors of antigens. The behavior of internalized antigens in APCs is crucial for the induction of immune responses. When antigens are taken up by APCs, they are usually localized into endosomes, and antigen-specific humoral immunity is induced when antigens remain in endosomes, while cellular immunity is induced when antigens escape from endosomes.⁸ In a previous study, we revealed that γ -PGA-AAE NPs showed membrane-disruptive activities at endosomal environment.²⁸ Therefore, OVA-NPs taken up by DCs should escape from endosomes after cellular uptake, and thus resulted in inducing a higher level of cellular immunity-biased immune response. On the other hand, the endosomal escape of OVA + NPs might not be efficient, and thus resulted in inducing a humoral immunity-biased immune response. The cellular uptake behaviors of antigens also affect the induction level of the immune response. The encapsulated OVA in γ -PGA-AAE NPs was efficiently taken up by DCs compared with OVA alone (Figure 4), while

the uptake amount of OVA + NPs was comparable with OVA alone (data not shown), and thus resulted in differences in the induction level of the immune response.

The hydrophobic segments affected the induction level of the cellular immunity, this may be due to differences in interactions (cellular uptake and activation potential) between γ -PGA-AAE NPs and DCs. Phe_{enc} induced higher cellular immunity than Trp_{enc}, and this result tended to repeat itself as the cellular uptake of OVA encapsulated into γ -PGA-AAE NPs (Figure 4a). On the other hand, Phe_{enc} induced higher cellular immunity than Leu_{enc}, which corresponds with the activation potential of OVA-NPs (Figure 5). The aforementioned results are schematically illustrated in Figure 9. Overall, the data

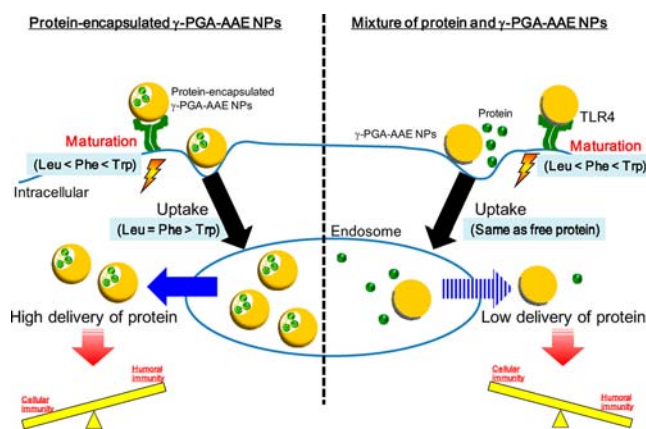


Figure 9. Schematic illustration of the effect of vaccine formulation and hydrophobic side chains of γ -PGA-AAE NPs on cellular interactions.

demonstrated that the cellular uptake of the encapsulated antigen, the type of induced immunity and/or induction level could be manipulated by changing the hydrophobic segment. γ -PGA-Leu NPs and γ -PGA-Phe NPs would be useful when the induction of an antigen-specific cellular immunity-biased immune response is required. For the mechanistic understanding of how hydrophobic segments affect the balance of induced immune response, elucidation of the intracellular behaviors of the encapsulated antigens should be essential. In a previous study, we revealed that the hydrophobicity of γ -PGA-Phe NPs affected the degradability of encapsulated antigens.³⁷ It has been reported that the induction efficiency of antigen-specific immune responses changed by the degradability of antigens loaded onto polymeric particles.³⁸ Taken altogether, although the surface hydrophobicity of γ -PGA-AAE NPs was the same (Figure 1), the hydrophobicity of each side chain (amino acid) was different. This should affect the degradability of encapsulated antigens, which might result in the difference in the induction level of the immune response. The size of NPs is also an important factor to control interactions with APCs, and biodistribution. In a previous study, the size of γ -PGA-Phe NPs affected the cellular uptake and the intracellular degradability of the encapsulated proteins,²¹ and migration behavior to the lymph nodes.²⁰ These results suggest that the intracellular behaviors and biodistribution of γ -PGA-AAE NPs could be controlled more precisely by changing the size, and might lead to a more efficient manipulation of the immune response. Nevertheless, our results demonstrated that hydrophobic segments in NPs significantly affect interactions with DCs,

and thus the balance of antigen-specific immune responses could be manipulated.

CONCLUSION

Amphiphilic γ -PGA copolymers were synthesized with various types of hydrophobic segments, and OVA-NPs were prepared from these copolymers. These NPs demonstrated low cytotoxicity and good biocompatibility. The cellular uptake of the encapsulated antigen and the activation behavior of DCs by OVA-NPs were changed by varying the kinds of hydrophobic segments. Moreover, the type and the induction level of the antigen-specific cellular and humoral immunities were manipulated by varying the vaccine formulation (encapsulation or mixture) and by varying the kinds of hydrophobic segments. When OVA was encapsulated into NPs, the cellular immunity was dominantly induced, while humoral immunity was dominant when OVA was mixed with NPs. These results are the first to report that the balance and induction level of cellular and humoral immunities could be controlled by modifying compositions of NPs and vaccine formulations. These data suggest that we could select suitable carriers for the protection from and/or treatment of infectious diseases, cancers, allergies, and autoimmune diseases. Our results suggest that γ -PGA-AAE NPs can provide safe and efficient nanoparticle-based vaccine adjuvants, and the results also provide guidelines for the rational design of amphiphilic polymers as vaccine adjuvants which can control the balance of immune responses.

EXPERIMENTAL SECTION

Materials. γ -PGA ($M_w = 500\,000$), 1,1,1,3,3,3-hexafluoro-2-propanol (HFIP), dimethyl sulfoxide (DMSO), and 1-ethyl-3-(3-(dimethylamino)propyl) carbodiimide (EDC), were purchased from Wako Pure Chemical Industries (Osaka, Japan). L-Leucine ethyl ester (Leu), L-phenylalanine ethyl ester (Phe), L-tryptophan ethyl ester (Trp), ovalbumin (OVA), RPMI 1640 medium, fetal bovine serum (FBS), and bovine serum albumin (BSA) were purchased from Sigma-Aldrich (MO, USA). FITC-labeled OVA (FITC-OVA) was purchased from Life Technologies (CA, USA). AddaVax (Adx) was purchased from InvivoGen (CA, USA). The antibiotics were purchased from Nacalai Tesque Inc. (Kyoto, Japan). Granulocyte macrophage colony stimulating factor (GM-CSF) was purchased from PeproTech (NJ, USA). Isoflurane was purchased from Abbott Japan Co. Ltd. (Tokyo, Japan). OVA_{257–264} peptide was synthesized by Operon Biotechnology Co. Ltd. (Tokyo, Japan). Horseradish peroxidase-conjugated anti-mouse IgG and IgE goat antibodies were purchased from Southern Biotechnology (AL, USA). 3,3',5,5'-Tetramethylbenzidine (TMB) substrate solution and TMB stop solution were purchased from Kirkegaard & Perry Laboratories, Inc. (MD, USA).

Synthesis of γ -PGA-AAE Copolymers. γ -PGA (3.1 unit mmol) was hydrophobically modified by Leu (3.4 mmol), Phe (3.1 mmol), or Trp (2.3 mmol) using EDC (3.4 mmol for Leu, 3.1 mmol for Phe, and 3.1 mmol for Trp) in 50 mM sodium hydrogen carbonate solution (60 mL) for 1 h on ice, and then for 24 h at room temperature.²⁸ The feeding ratio of Leu, Phe, or Trp to γ -PGA was 1:1.1, 1:1, or 1:0.75, respectively. Synthesized γ -PGA-AAE copolymers were then dialyzed against water for 5 days and freeze-dried for 3 days. γ -PGA-AAE copolymers were confirmed by FT-IR spectroscopy (Spectrum

100, PerkinElmer, USA) and ^1H NMR (ECS-400, JEOL, Japan).

Hydrophobicity Measurements. Hydrophobicity of γ -PGA-AAE copolymers was evaluated by measuring water contact angles. γ -PGA-AAE (10 mg/mL in HFIP, 0.5 mL) was coated onto glass slides with a spin coater (Spincoater 1H-D7, Mikasa, Co., Ltd., Japan) at 1500 rpm, and contact angles were evaluated using a DropMaster 500 (Kyowa Interface Science Co., Ltd., Japan). Contact angles were measured after water droplets (0.5 μL) were cast onto substrates and placed for 5 s. The contact angle of each sample was measured 10 times.

Preparation of γ -PGA-AAE NPs and Protein-Encapsulated γ -PGA-AAE NPs. γ -PGA-AAE NPs were prepared according to methods described in a previous report.²⁹ Briefly, γ -PGA-AAE (10 mg/mL in DMSO) was added to an equal volume of sodium chloride (NaCl) solution. The size of γ -PGA-AAE NPs was regulated by changing the salt concentration. The resulting solutions were dialyzed for 3 days to remove DMSO and salt. γ -PGA-AAE NPs were then dispersed into phosphate-buffered saline (PBS). In this study, OVA was used as a model antigen to evaluate the induction of antigen-specific immune responses. FITC-OVA was also used to evaluate the cellular uptake of encapsulated proteins. To prepare OVA-NPs or FITC-OVA-NPs, γ -PGA-AAE (10 mg/mL in DMSO) was added to an equal volume of OVA or FITC-OVA solution (875 $\mu\text{g/mL}$).²⁹ The sizes of OVA-NPs or FITC-OVA-NPs were adjusted by the salt concentration. The resulting solution was dialyzed for 2 days and then dispersed into PBS. The size distributions and zeta potentials of these NPs were measured by a dynamic light scattering (DLS) method using a Zetasizer Nano ZS (Malvern Instruments, UK). The amount of the encapsulated OVA was measured with the Lowry method by dissolving OVA-NPs with 2% sodium dodecyl sulfate (SDS). The amount of the encapsulated FITC-OVA was measured by the fluorescence intensity.

Mice. Female C57BL/6J (H-2K^b, 6–8 weeks of age) mice were purchased from CLEA Japan (Tokyo, Japan). All experiments were approved by Osaka University and were carried out in accordance with the institutional guidelines for animal experimentation.

Preparation of DCs. Bone marrow-derived DCs were generated, as previously reported.³⁰ Briefly, femurs and tibias were removed from mice, both ends of the bones were cut with scissors, and the bone marrow was flushed with PBS using a syringe with a 26-gauge needle. The suspension was passed through a 50 μm cell strainer (BD Bioscience). Cells (2.5×10^6 cells/10 mL) were suspended in RPMI 1640 medium supplemented with 10% heat-inactivated FBS, 1% antibiotics, and 20 ng/mL recombinant mouse GM-CSF and placed into a bacteriological Petri dish. Fresh culture medium was added to the dish on day 3. On day 7, the non-adherent or loosely adherent cells were harvested and used as DCs.

Cytotoxicity Test of γ -PGA-AAE NPs. To evaluate the cytotoxicity of γ -PGA-AAE NPs and OVA-NPs, DCs were seeded into 48-well plates at 5×10^5 cells/well with γ -PGA-AAE NPs (500 $\mu\text{g/mL}$) or OVA-NPs (20 $\mu\text{g/mL}$ OVA, 500 $\mu\text{g/mL}$ NPs) and incubated for 24 h. DCs were then collected, and viability was evaluated by staining with trypan blue dye.

Cellular Uptake of FITC-OVA-NPs by DCs. To evaluate the effect of side chains of NPs on the cellular uptake by DCs, FITC-OVA was used. DCs (1×10^6 cells/mL) were incubated with FITC-OVA (4 $\mu\text{g/mL}$) or FITC-OVA-NPs (4 $\mu\text{g/mL}$

FITC-OVA and 100 $\mu\text{g/mL}$ NPs) for determined time periods at 37 °C. Cells were washed with PBS, and the cell-associated fluorescence was measured by flow cytometry (Cytomics FC500, Beckman Coulter, US). The cellular uptake of FITC-OVA-NPs after 180 min incubation was also observed using a confocal fluorescence microscopy (DSU-IX81-SET fluorescence microscope, Olympus, Japan).

Stimulation of DCs by γ -PGA-AAE NPs and OVA-NPs.

DCs were seeded into 48-well plates at 5×10^5 cells/well with γ -PGA-AAE NPs (500 $\mu\text{g/mL}$), OVA (20 $\mu\text{g/mL}$), or OVA-NPs (20 $\mu\text{g/mL}$ OVA and 500 $\mu\text{g/mL}$ NPs) and incubated for 24 h at 37 °C. To analyze cytokine production, supernatants were collected, and amounts of TNF- α secreted were measured by an enzyme-linked immunosorbent assay (ELISA) (Life Technologies, CA, USA).

Immunization of Mice and Histopathological Examination of Injection Site. Mice were anesthetized by isoflurane and immunized with OVA-NPs or OVA + NPs. The mice (three mice per group) were immunized subcutaneously twice with PBS, OVA, OVA-NPs, OVA + NPs, or OVA + Adx on days 0 and 7. Adx is known as a squalene-based oil-in-water nanoemulsion based on the formulation of MF59 that has been licensed in Europe for adjuvanted flu vaccines.³¹ The amounts of injected OVA and γ -PGA-AAE NPs were fixed at 10 μg and 200 μg per injection, respectively. On day 14 following the first immunization, spleen cells and blood were collected. Spleen cells collected from each group of mice were pooled and the immune response was evaluated. The histopathological examination of injection sites was also conducted. After final immunization, subcutaneous tissues were collected, fixed with 4% paraformaldehyde phosphate buffer solution, and embedded in paraffin. Sections (5 μm) were prepared for hematoxylin and eosin staining. Histopathological examinations were performed at the Applied Medical Research Laboratory, Osaka, Japan.

ELISPOT Assay. Interferon (IFN)- γ -producing cells were determined using an enzyme-linked immunospot (ELISPOT) kit for mouse IFN- γ (BD Biosciences, CA, USA). Lymphocyte cells were isolated by density-gradient centrifugation, and cells (2×10^5 cells/well) were stimulated with OVA_{257–264} peptide (1 $\mu\text{g/mL}$) in a 96-well ELISPOT plate. Plates were incubated for 24 h at 37 °C, washed, and further incubated with a biotin-conjugated detection antibody for 2 h at room temperature. After washing, plates were incubated with streptavidin-conjugated horse radish peroxidase and incubated for 1 h. Plates were washed and incubated with substrate for 15 min. The colorimetric reaction was terminated by washing with water. After the plates were dried, the number of spots was counted using a microscope.

ELISA. Sera were examined for anti-OVA antibody (Ab) titers by ELISA. Briefly, flat-bottomed 96-well Nunc MaxiSorp plates (Thermo Scientific, MA, USA) were coated with OVA suspended in carbonate–bicarbonate buffer (1 $\mu\text{g/mL}$) and subjected to overnight incubation at 4 °C. Plates were washed with T-PBS (0.05% Tween 20 in PBS) and incubated with blocking buffer (1% BSA and 1% skim milk in T-PBS) for 2 h at room temperature. Serum samples diluted with blocking buffer were added to each well. After incubation for 2 h at room temperature, plates were incubated with a horseradish peroxidase-conjugated anti-mouse IgG or IgE goat Ab. Plates were developed by adding TMB substrate to each well and incubated for 10 min. Colorimetric reactions were terminated by adding TMB stop solution, and the absorbance of each well

was measured at 450 nm by a microplate reader (xMark, Microplate Spectrophotometer, BioRad, USA). End point titers were determined by optical density of 0.1.

AUTHOR INFORMATION

Corresponding Author

*E-mail: akashi@chem.eng.osaka-u.ac.jp.

Notes

The authors declare no competing financial interest.

ACKNOWLEDGMENTS

This work was supported by a Research Fellow of the Japan Society for the Promotion of Science and a Grant-in-Aid for Scientific Research (S) from the Ministry of Education, Culture, Sports, Science, and Technology (23225004).

ABBREVIATIONS

APCs, antigen presenting cells; DCs, dendritic cells; NPs, nanoparticles; MHC, major histocompatibility complex; CTL, cytotoxic T lymphocyte; OVA, ovalbumin; γ -PGA, poly(γ -glutamic acid); AAE, amino acid ethyl ester; Leu, leucine ethyl ester; Phe, L-phenylalanine ethyl ester; Trp, tryptophan ethyl ester; TLR, Toll-like receptor; OVA-NPs, OVA-encapsulated γ -PGA-AAE NPs; FITC-OVA-NPs, FITC-OVA-encapsulated γ -PGA-AAE NPs; OVA + NPs, mixture of OVA and γ -PGA-AAE NPs; Leu_{enc}, OVA-encapsulated γ -PGA-Leu NPs; Phe_{enc}, OVA-encapsulated γ -PGA-Phe NPs; Trp_{enc}, OVA-encapsulated γ -PGA-Trp NPs; Leu_{mix}, mixture of OVA and γ -PGA-Leu NPs; Phe_{mix}, mixture of OVA and γ -PGA-Phe NPs; Trp_{mix}, mixture of OVA and γ -PGA-Trp NPs; OVA-Adx, mixture of OVA and Adx; Ab, antibody; TNF- α , tumor necrosis factor α ; INF- γ , interferon γ

REFERENCES

- (1) Peek, L. J., Middaugh, C. R., and Berkland, C. (2008) Nanotechnology in vaccine delivery. *Adv. Drug Delivery Rev.* 60, 915–928.
- (2) O'Hagan, D. T., and Valiante, N. M. (2003) Recent advances in the discovery and delivery of vaccine adjuvants. *Nat. Rev. Drug Discovery* 2, 727–735.
- (3) Hubbell, J. A., Thomas, S. N., and Swartz, M. A. (2009) Materials engineering for immunomodulation. *Nature* 462, 449–460.
- (4) Swartz, M. A., Hirose, S., and Hubbell, J. A. (2012) Engineering approaches to immunotherapy. *Sci. Transl. Med.* 4, 148rv9.
- (5) Moon, J. J., Huang, B., and Irvine, D. J. (2012) Engineering nano- and microparticles to tune immunity. *Adv. Mater.* 24, 3724–3746.
- (6) Foged, C., Sundblad, A., and Hovgaard, L. (2002) Targeting vaccines to dendritic cells. *Pharm. Res.* 19, 229–238.
- (7) Kanchan, V., and Panda, A. K. (2007) Interactions of antigen-loaded polylactide particles with macrophages and their correlation with the immune response. *Biomaterials* 28, 5344–5357.
- (8) Neeffes, J., Jongsma, M. L. M., Paul, P., and Bakke, O. (2011) Towards a systems understanding of MHC class I and MHC class II antigen presentation. *Nat. Rev. Immunol.* 11, 823–836.
- (9) Heath, W. R., and Carbone, F. R. (2001) Cross-presentation in viral immunity and self-tolerance. *Nat. Rev. Immunol.* 1, 126–135.
- (10) Kreuter, J., Liehl, E., Berg, U., Soliva, M., and Speiser, P. P. (1988) Influence of hydrophobicity on the adjuvant effect of particulate polymeric adjuvants. *Vaccine* 6, 253–256.
- (11) Seong, S. Y., and Matzinger, P. (2004) Hydrophobicity: an ancient damage-associated molecular pattern that initiate immune responses. *Nat. Rev. Immunol.* 4, 469–478.
- (12) Chiu, Y. L., Ho, Y. C., Chen, Y. M., Peng, S. F., Ke, C. J., Chen, K. J., Mi, F. L., and Sung, H. W. (2010) The characteristics, cellular

uptake and intracellular trafficking of nanoparticles made of hydrophobically-modified chitosan. *J. Controlled Release* 146, 152–159.

(13) Moyano, D. F., Goldsmith, M., Solfiell, D. J., Milo, D. L., Miranda, O. R., Peer, D., and Rotello, V. M. (2012) Nanoparticle hydrophobicity dictates immune response. *J. Am. Chem. Soc.* 134, 3965–3967.

(14) Murthy, N., Robichaud, J. R., Tirrell, D. A., Stayton, P. S., and Hoffman, A. S. (1999) The design and synthesis of polymers for eukaryotic membrane disruption. *J. Controlled Release* 61, 137–143.

(15) Jones, R. A., Cheung, C. Y., Black, F. E., Zia, J. K., Stayton, P. S., Hoffman, A. S., and Wilson, M. R. (2003) Poly(2-alkylacrylic acid) polymers deliver molecules to the cytosol by pH-sensitive disruption of endosomal vesicles. *Biochem. J.* 372, 65–75.

(16) Uto, T., Toyama, M., Nishi, Y., Akagi, T., Shima, F., Akashi, M., and Baba, M. (2013) Uptake of biodegradable poly(γ -glutamic acid) nanoparticles and antigen presentation by dendritic cells in vivo. *Results Immunol.* 3, 1–9.

(17) Shima, F., Uto, T., Akagi, T., and Akashi, M. (2013) Synergistic stimulation of antigen presenting cells via TLR by combining CpG ODN and poly(γ -glutamic acid)-based nanoparticles as vaccine adjuvants. *Bioconjugate Chem.* 24, 926–933.

(18) Uto, T., Akagi, T., Toyama, M., Nishi, Y., Shima, F., Akashi, M., and Baba, M. (2011) Comparative activity of biodegradable nanoparticles with aluminum adjuvants: antigen uptake by dendritic cells and induction of immune response in mice. *Immunol. Lett.* 140, 36–43.

(19) Uto, T., Akagi, T., Yoshinaga, K., Toyama, M., Akashi, M., and Baba, M. (2011) The induction of innate and adaptive immunity by biodegradable poly(γ -glutamic acid) nanoparticles via a TLR4 and MyD88 signaling pathway. *Biomaterials* 32, 5206–5212.

(20) Shima, F., Uto, T., Akagi, T., Baba, M., and Akashi, M. (2013) Size effect of amphiphilic poly(γ -glutamic acid) nanoparticles on cellular uptake and maturation of dendritic cells in vivo. *Acta Biomater.* 9, 8894–8901.

(21) Akagi, T., Shima, F., and Akashi, M. (2011) Intracellular degradation and distribution of protein-encapsulated amphiphilic poly(amino acid) nanoparticles. *Biomaterials* 32, 4959–4967.

(22) Shima, F., Akagi, T., Uto, T., and Akashi, M. (2013) Manipulating the antigen-specific immune response by the hydrophobicity of amphiphilic poly(γ -glutamic acid) nanoparticles. *Biomaterials* 34, 9709–9716.

(23) Shima, F., Akagi, T., and Akashi, M. (2013) The role of hydrophobicity in the disruption of erythrocyte membrane by nanoparticles composed of hydrophobically modified poly(γ -glutamic acid). *J. Biomater. Sci. Polym. Ed.* 25, 203–210.

(24) Tayar, N. E., Tsai, R. S., Carrupt, P. A., and Testa, B. (1992) Octan-1-ol-water partition coefficients of zwitterionic α -amino acids. Determination by centrifugal partition chromatography and factorization into steric/hydrophobic and polar components. *J. Chem. Soc., Perkin. Trans. 2*, 79–84.

(25) Csizmadia, F., Tsantili-Kakoulidou, A., Panderi, I., and Darvas, F. (1997) Prediction of distribution coefficient from structure. I. Estimation method. *J. Pharm. Sci.* 86, 865–871.

(26) Ohmori, N., Niidome, T., Kiyota, T., Lee, S., Sugihara, G., Wada, A., Hirayama, T., and Aoyagi, H. (1998) Importance of Hydrophobic Region in Amphiphilic Structures of α -Helical Peptides for Their Gene Transfer-Ability into Cells. *Biochem. Biophys. Res. Commun.* 245, 259–265.

(27) Li, W., Nicol, F., and Szoka, F. C., Jr (2004) GALA: a designed synthetic pH-responsive amphipathic peptide with applications in drug and gene delivery. *Adv. Drug Delivery Rev.* 56, 967–985.

(28) Shima, F., Akagi, T., and Akashi, M. (2014) Synthesis and preparation of nanoparticles composed of amphiphilic poly(γ -glutamic acid) with different hydrophobic side chains and their potential of membrane disruptive activity. *Colloid Polym. Sci.* 292, 2663–2671.

(29) Kim, H., Akagi, T., and Akashi, M. (2009) Preparation of size tunable amphiphilic poly(amino acid) nanoparticles. *Macromol. Biosci.* 9, 842–848.

(30) Uto, T., Wang, X., Sato, K., Haraguchi, M., Akagi, T., Akashi, M., and Baba, M. (2007) Targeting of antigen to dendritic cells with

poly(γ -glutamic acid) nanoparticles induces antigen-specific humoral and cellular immunity. *J. Immunol.* 178, 2979–2986.

(31) Mbow, M. L., Gregorio, E. D., Valiante, N. M., and Rappuoli, R. (2010) New adjuvants for human vaccines. *Curr. Opin. Immunol.* 22, 411–416.

(32) Liu, Y., Yin, Y., Wang, L., Zhang, W., Chen, X., Yang, X., Xu, J., and Ma, G. (2013) Surface hydrophobicity of microparticles modules adjuvanticity. *J. Mater. Chem. B* 1, 3888–3896.

(33) Lacey, M. H., Bramwell, V. W., Christensen, D., Agger, E. M., Andersen, P., and Perrie, Y. (2010) Liposomes based on dimethyldioctadecylammonium promote a depot effect and enhance immunogenicity of soluble antigen. *J. Controlled Release* 142, 180–186.

(34) Lacey, M. H., Christensen, D., Bramwell, V. M., Lindström, L., Agger, E. M., Andersen, P., and Perrie, Y. (2011) Comparison of the depot effect and immunogenicity of liposomes based on dimethyldioctadecylammonium (DDA), 3 β -[N-(N',N'-dimethylaminoethane)carbonyl] cholesterol (DC-Chol), and 1,2-dioleoyl-3-trimethylammonium propane (DOTAP): prolonged liposome retention mediates stronger Th1 responses. *Mol. Pharmaceutics* 8, 153–161.

(35) Yi, A. K., Yoon, J. G., Hong, S. C., Redford, T. W., and Krieg, A. M. (2001) Lipopolysaccharide and CpG DNA synergize for tumor necrosis factor- α production through activation of NF- κ B. *Int. Immunol.* 13, 1391–1404.

(36) Lee, T. Y., Kim, Y. H., Yoon, S. W., Choi, J. C., Yang, J. M., Kim, C. J., Schiller, J. T., Sung, M. H., and Poo, H. (2009) Oral administration of poly-gamma-glutamate induces TLR4-and dendritic cell-dependent antitumor effect. *Cancer Immunol. Immunother.* 58, 1781–1794.

(37) Shima, F., Akagi, T., and Akashi, M. (2014) The hydrophobic effect of nanoparticles composed of amphiphilic poly(γ -glutamic acid) on the degradability of the encapsulated proteins. *Biomater. Sci.* 2, 1419–1425.

(38) Tran, K. K., and Shen, H. (2009) The role of phagosomal pH on the size-dependent efficiency of cross-presentation by dendritic cells. *Biomaterials* 30, 1356–1362.